AIP | Review of Scientific Instruments

Microwave Doppler reflectometer system in LHD

T. Tokuzawa, A. Ejiri, K. Kawahata, K. Tanaka, I. Yamada et al.

Citation: Rev. Sci. Instrum. **83**, 10E322 (2012); doi: 10.1063/1.4733736
View online: http://dx.doi.org/10.1063/1.4733736
View Table of Contents: http://rsi.aip.org/resource/1/RSINAK/v83/i10
Published by the American Institute of Physics.

Microwave Doppler reflectometer system in LHD[a)]

T. Tokuzawa,[1,b)] A. Ejiri,[2] K. Kawahata,[1] K. Tanaka,[1] I. Yamada,[1] M. Yoshinuma,[1] K. Ida,[1] and C. Suzuki[1]
[1]*National Institute for Fusion Science, 322-6 Oroshi-cho, Toki 509-5292, Japan*
[2]*Graduate School of Frontier Sciences, The University of Tokyo, Kashiwa 277-8561, Japan*

(Presented 7 May 2012; received 7 May 2012; accepted 18 June 2012; published online 13 July 2012)

In order to measure the poloidal rotation velocity, a Doppler reflectometer has been developed in Large Helical Device (LHD). A remotely controlled antenna tilting system has been installed in an LHD vacuum vessel. A synthesizer is used as the source, and the operation microwave frequency ranges are *ka*-band and *V*-band. In LHD last experimental campaign we obtained the Doppler shifted signal, which was consistent with CXRS measurements. © *2012 American Institute of Physics*. [http://dx.doi.org/10.1063/1.4733736]

I. INTRODUCTION

Doppler reflectometry is a unique technique when used in combination with the back-scattering method and reflectometry. Recently, a number of systems have been used in devices throughout the world, such as tokamaks (Tuman-3M,[1] ASDEX Upgrade,[2,3] Tore Supra,[4] DIII-D,[5] JT-60U (Ref. 6)) and helical/stellarators (Wendelstein 7-AS,[7,8] TJ-II (Ref. 9)). Doppler reflectometry can measure the perpendicular velocity of electron density fluctuations $v_\perp$, the radial electric field E_r, and the perpendicular wave number spectrum $S(k_\perp)$ in magnetized confinement plasmas. In particular, E_r and its shear are important parameters for understanding plasma turbulence and confinement transition phenomena.

The principle of Doppler reflectometry can be explained by the grating reflection model with small sinusoidal corrugation characterized by wave number $k_\perp$. The signal wave is launched and received under a non-zero tilt angle $\theta_{\rm tilt}$ with respect to the normal to the reflecting layer. Thus, this measurement selects perturbations with a finite wave vector component on the reflecting layer $k_\perp$ via microwave scattering to diffraction order of -1. This condition determines the probed wave number to $k_\perp = -2k_{\rm i}$, where $k_{\rm i}$ is the local wave vector of the incident beam. For a plasma slab, the Bragg condition $k_{\rm i} = k_0 \sin(\theta_{\rm tilt})$, where k_0 is the wave number of microwaves in a vacuum. By scanning $\theta_{\rm tilt}$, the $k_\perp$-spectrum of the density perturbations can be obtained. The unwanted strong 0th order reflection used in conventional reflectometry is at least partially suppressed as the finite tilting angle causes the propagating direction to shift out of the receiving antenna pattern. For the high-curvature LHD plasma, the perpendicular wave number is determined from $k_\perp = -2k_{\rm i}$, where $k_{\rm i}$ is calculated by the LHDGAUSS (Ref. 10) 3D beam tracing code.

The Doppler shift of the received signal depends on the velocity of the plasma turbulence, and its wave number is expressed as

$$\omega_D = \mathbf{v}\cdot\mathbf{k} = v_\perp k_\perp + v_{||}k_{||} + v_r k_r, \tag{1}$$

where v is the velocity and its subscript $_{||}$ and r indicate parallel and radial, respectively. In magnetically confined plasmas, it can usually be assumed that $k_\perp \gg k_{||}$ and $v_\perp < v_{||}$, so that the second term is negligible in comparison with the first term. If, in addition, the turbulence does not displace itself radially, the third term vanishes, and $\omega_{\rm D} = v_\perp k_\perp$ is obtained. The perpendicular propagation velocity $v_\perp(k_\perp)$ of the selected perturbations can be calculated. The perpendicular propagation velocity is a composition of the plasma background *ExB* velocity $v_{\rm ExB}$ and the intrinsic phase velocity of the density fluctuations $v_{\rm ph}$. This relation is $v_\perp = v_{E\times B} + v_{ph}$. At the plasma edge, $v_{\rm ph} \ll v_{\rm ExB}$ is usually satisfied in magnetically confined devices. Then, the radial electric field E_r can be deduced from the measurement of the perpendicular velocity through $E_r = v_\perp B$, where B is the absolute value of the magnetic field.

In the present paper we describe the diagnostics system status in Sec. II and present the first experimental results in Sec. III.

II. MICROWAVE DIAGNOSTIC SYSTEM SETUP

A. Antenna design

In order to achieve a sufficient back-scattered measurement configuration, the launching/receiving antennae are installed in a vacuum vessel, as shown in Fig. 1. In addition, the optimized wave number measurement requires the remote control structure of the antenna. In this antenna system, the tilting angle can be changed from 0° to 32° in less than 2 min. The antenna system consists of a straight circular corrugated waveguide and combination focusing mirrors. The launching microwave is a quasi-Gaussian wave. The beam pattern at the plasma edge is shown in Fig. 2. The frequency of the test is 39 GHz, and the beam width is ~26 mm. The theoretical wave number spectral resolution of the Gaussian beam can be written as follows:

$$\Delta k_\perp = \frac{2\sqrt{2}}{\omega}\sqrt{1+\left(\frac{\omega^2 k_0}{\rho_{eff}}\right)^2}, \tag{2}$$

[a)]Contributed paper, published as part of the Proceedings of the 19th Topical Conference on High-Temperature Plasma Diagnostics, Monterey, California, May 2012.

[b)]Author to whom correspondence should be addressed. Electronic mail: tokuzawa@nifs.ac.jp.

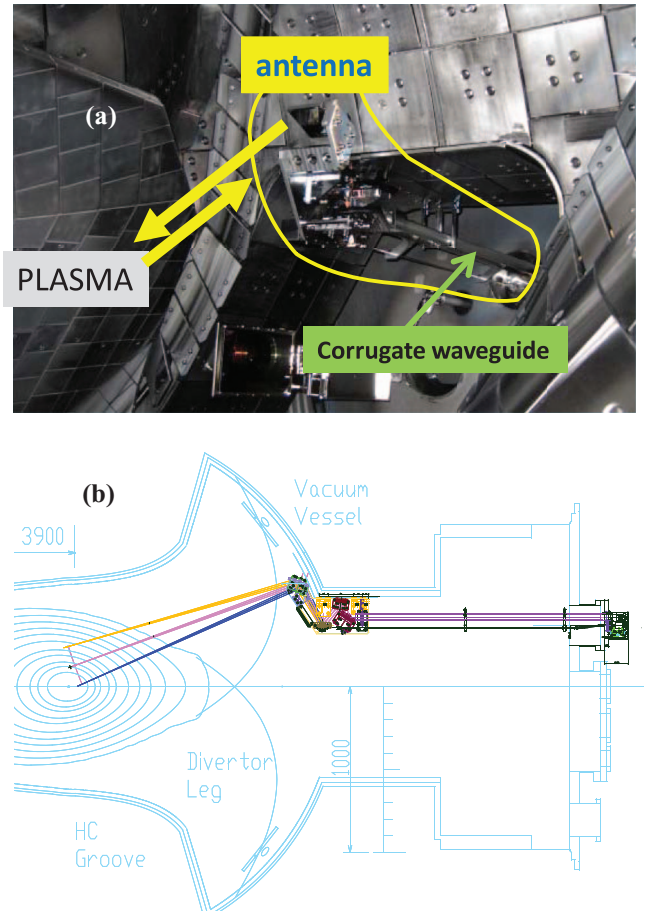

FIG. 1. (a) Photograph of in-vessel antenna configuration and (b) cross section design of LHD vacuum vessel and Doppler reflectometer antenna system.

where $\Delta k_\perp$ is the $1/e$-width of the amplitude spectrum, ω is the beam radius, $\rho_{\text{eff}} = R_{\text{plasma}}R_{\text{beam}}/(R_{\text{plasma}} + R_{\text{beam}})$ is the effective radius of curvature, and R_{plasma} and R_{beam} are the curvature radii of the plasma and the launching microwave beam, respectively. The optimal spectral resolution is ~ 2 cm^{-1} in this system.

In order to obtain the radial scattering position and the perpendicular wave number $k_\perp$, the LHDGAUSS three-dimensional beam tracing code is used. The wave numbers perpendicular to $k_\perp$ and parallel to $k_\parallel$ the magnetic field at each point of the ray trajectory are calculated. The measured wave number of the density fluctuation is then obtained at the ray turning point. In Fig. 3(b) the radial dependence of the perpendicular wave number $k_\perp$ is shown. Here, each point is calculated under the condition of a different launching angle θ and frequency in the assumed parabolic density profile shown in Fig. 3(a). In this case, we can measure the perpendicular wave number $k_\perp$ to be up to 15 cm^{-1} with an optimized alignment of the antenna and launching frequency. Of course, there is a very wide variety of LHD plasmas. Sometimes, the density is higher and the corresponding scattering point moves outside and the measurable area is reduced.

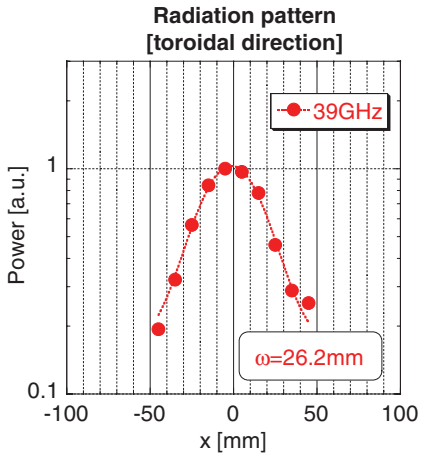

FIG. 2. Radiation pattern for $f = 39$ GHz. The dotted line shows the Gaussian fitting result. The beam width is about 26 mm.

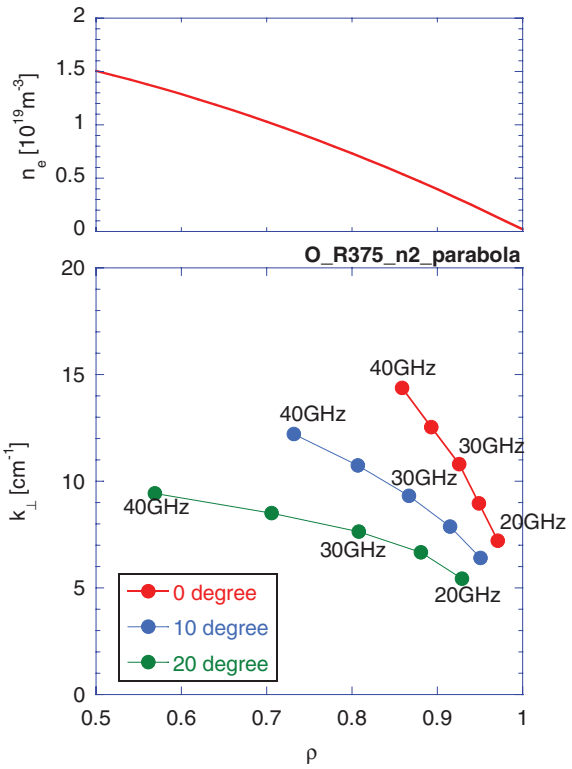

FIG. 3. (a) Assumed parabolic density profile and (b) dependence of perpendicular wave number $k_\perp$ on the radius ρ, different launch angles θ, and frequency calculated by LHDGAUSS code.

B. Microwave circuit

We have constructed both *ka*-band and *V*-band systems. In the present paper, we concentrate on explaining the *ka*-band system. A schematic diagram of the *ka*-band Doppler reflectometer system is shown in Fig. 4. A microwave synthesizer is used as a source because its phase noise is low enough to apply the density fluctuation measurements. In addition, this output is divided in order to use the source of the *V*-band system. The frequency range is from 13 to 20 GHz, and its output frequency is easily changed by the external GPIB control. The source output is split into the probe signal and the reference signal. The probe signal is doubled followed by an active multiplier in order to bring the launching frequency up to 26 to 40 GHz (*ka*-band). The microwave launches from the outboard side along the inverse of the major radius

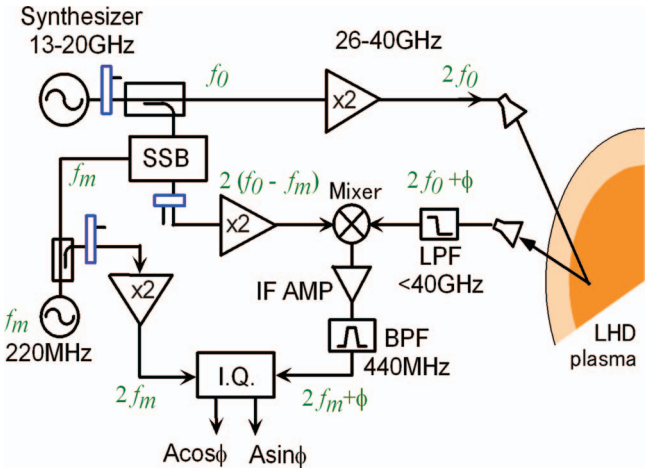

FIG. 4. Schematic diagram of the *ka*-band Doppler reflectometer system.

direction with tilting angle. The polarization of the launching wave can be selected as either the ordinary mode or extraordinary mode. The returning scattered wave is received and mixed with the reference wave. In order to obtain the complex frequency components and the phase fluctuation, single sideband (SSB) modulation is used.[11] The SSB modulator, which is driven by a 220 MHz (f_m) quartz oscillator, shifts the frequency of the reference signal for heterodyne I-Q detection. The suppression levels of the image sidebands are less than −20dB in this system. The intermediate frequency (IF) signal is amplified and filtered by a band pass filter (BPF), the pass frequency component of which is 440 ± 10 MHz. The IF signal and the modulation signal are then led to the I-Q detector. The output signals of the I-Q demodulator, which are denoted as $A\cos\phi$ and $A\sin\phi$, are acquired using a real-time data acquisition system consisting of two compact PCI digitizers, the sampling rates of which are 1 and 10 MHz throughout plasma discharge. In addition, the part of the IF signal is measured by a spectrum analyzer in order to monitor the frequency shift.

III. EXPERIMENTAL RESULTS

Here, we explain the preliminary LHD plasma experimental results of this Doppler reflectometer system. First, we investigate the direction of the back-scattered wave. We believe that when the direction of the LHD magnetic field is changed, the sign of the Doppler shift frequency would be changed. Two discharges, the heating power and most of the plasma parameters of which are approximately the same, are used for this purpose. The density profiles shown in Fig. 5(c) are approximately the same in the edge region. Figure 5(a) shows the complex frequency spectra measured in the positive magnetic field discharge, the magnetic axis position R_{ax} and axial magnetic field strength B_t of which are 3.60 m and 2.75 T, respectively. Figure 5(b) shows the negative magnetic field direction case, in which R_{ax} is 3.575 m and B_t is −2.769 T. The Doppler shift peak moves to the ion diamagnetic direction in both cases. The Doppler shifted peak frequency is estimated by the Gaussian fitting curve and is −123.2 ± 2.6 kHz in the positive magnetic field discharge case and 96.9 ± 2.7 kHz in the negative magnetic field discharge case. The radial profiles of poloidal velocity measured by charge

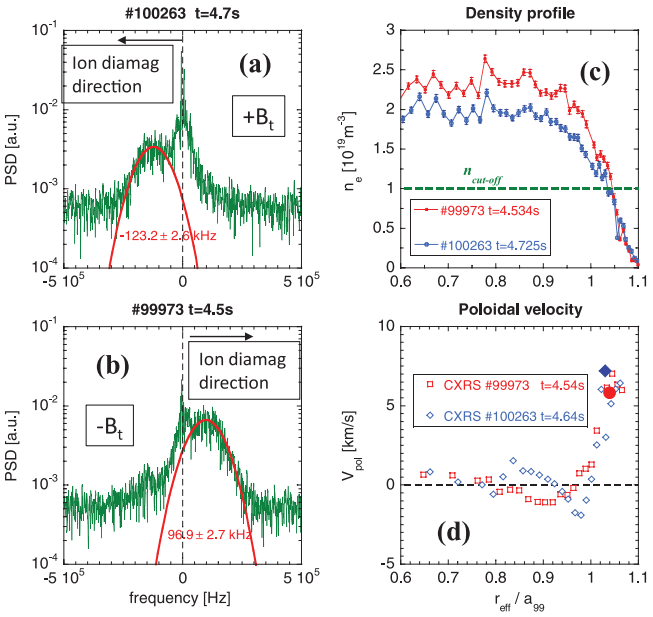

FIG. 5. Complex frequency spectra. Each magnetic field direction is positive (a) and negative (b). Solid (red) lines show the Gaussian fitting curve for extracting the Doppler shift. Radial profiles of (c) electron density measured by Thomson scattering and (d) poloidal velocity measured by charge exchange spectroscopy. Also, the estimated poloidal velocities from Doppler shift frequency are over-plotted in (d). Closed circle is #99973 data and diamond is #100263 data, respectively.

exchange recombination spectroscopy (CXRS) are shown in Fig. 5(d). Using the Doppler shift frequency, the poloidal velocities are estimated to be ∼7.2 km/s (#100263) in the positive magnetic field discharge case and 5.8 km/s (#99973) in the negative magnetic field discharge case. These values are quite reasonable compared with the CXRS data. In addition, the scattered signal is not so strong currently. This makes the delicate determination of Doppler shift especially difficult in the low-velocity range. One reason for this is that the source power is insufficient because one source is used for two systems. We intend address this problem in the near future.

ACKNOWLEDGMENTS

The present study was supported in part by KAKENHI (Grant Nos. 22360394 and 22017007) and by a Grant-in-Aid from the NIFS LHD project under the auspices of the NIFS Collaboration Research Program. Additional support was provided by Japan/U.S. Cooperation in Fusion Research and Development.

[1] V. V. Bulanin *et al.*, Plasma Phys. Rep. **26**, 813 (2000).
[2] G. D. Conway *et al.*, Plasma Phys. Controlled Fusion **46**, 951 (2004).
[3] J. Schirmer *et al.*, Plasma Phys. Controlled Fusion **49**, 1019 (2007).
[4] P. Hennequin *et al.*, Rev. Sci. Instrum. **75**, 3881 (2004).
[5] J. C. Hillesheim *et al.*, Rev. Sci. Instrum. **80**, 083507 (2009).
[6] N. Oyama *et al.*, Plasma Fusion Res. **6**, 1402014 (2011).
[7] M. Hirsch *et al.*, Rev. Sci. Instrum. **72**, 324 (2001).
[8] M. Hirsch *et al.*, Plasma Phys. Controlled Fusion **43**, 1641 (2001).
[9] T. Happel *et al.*, Rev. Sci. Instrum. **80**, 073502 (2009).
[10] S. Kubo *et al.*, "ECH power deposition study in the collisonless plasma of LHD," in *Proceedings of 11th International Congress on Plasma Physics, Sydney, Australia, July 2002* (AIP Conf. Proc.) **669**, 187.
[11] T. Tokuzawa *et al.*, Rev. Sci. Instrum. **79**, 10F109 (2008).